Yong Group Research Notes

Jonathan Shao-Kai Huang

September 11, 2025

Abstract

2025 Yong's Quantum Light Matter Group

Jonathan Shao-Kai Huang[1]

[1]) Department of Physics, National Taiwan University

Contents

Chapter 1

Nonlinear Optics

1.1 Classical Optics

Maxwell's equations are fundamentally linear. In standard units, they are given by four partial differential equations

$$\begin{aligned} \nabla \cdot \mathbf{E} &= \frac{\rho}{\epsilon_0} \\ \nabla \cdot \mathbf{B} &= 0 \\ \nabla \times \mathbf{E} &= -\frac{\partial \mathbf{B}}{\partial t} \\ \nabla \times \mathbf{B} &= \mu_0 \mathbf{J} + \mu_0 \epsilon_0 \frac{\partial \mathbf{E}}{\partial t}. \end{aligned} \tag{1.1}$$

We have linear constitutive relations

$$\begin{aligned} \mathbf{D} &= \epsilon_0 \mathbf{E} + \mathbf{P} \\ \mathbf{P} &= \chi \epsilon_0 \mathbf{E}. \end{aligned} \tag{1.2}$$

However, in the presence of matter, nonlinear effects arise and must be accounted for. We can write

$$\mathbf{P} = \epsilon_0 \chi^{(1)} \mathbf{E} + \mathbf{P}_{\mathrm{NL}} = \epsilon_0 \chi^{(1)} \mathbf{E} + \chi^{(2)} \mathbf{E}^2 + \chi^{(3)} \mathbf{E}^3 + \dots. \tag{1.3}$$

1.1.1 Anharmonic Oscillator

The electric field of monochromatic light can be written as

$$\mathbf{E}(t) = \frac{1}{2} \left[\mathbf{E}(\omega) e^{-i\omega t} + \mathbf{E}^*(-\omega) e^{i\omega t} \right], \tag{1.4}$$

where $\mathbf{E}(\pm\omega)$ is the amplitude, ω is the carrier frequency, and $\mathbf{E}(-\omega)$ is the negative-frequency component. By reality of $\mathbf{E}$, we have $\mathbf{E}^*(-\omega) = \mathbf{E}^*(\omega)$. Therefore, we simply redefine $\mathbf{E}(\omega)$ and use

$$\mathbf{E}(t) = \mathbf{E}(\omega) e^{-i\omega t}. \tag{1.5}$$

A simple model for light-matter interaction is the **Lorentz oscillator model**, which treats the electrons as damped classical oscillators and assumes harmonic fields. The equation of motion for a bound electron is given by

$$\frac{\mathrm{d}^2 \mathbf{r}}{\mathrm{d}t^2} + \frac{1}{\tau} \frac{\mathrm{d}\mathbf{r}}{\mathrm{d}t} + \omega_0^2 \mathbf{r} = -\frac{e}{m} E(t). \tag{1.6}$$

Here $\mathbf{r}$ is the displacement of the electron from rest position, τ is the relaxation time, and ω_0 is the resonance frequency of the oscillator. For time-harmonic fields, assume $\mathbf{E}(t) = \mathbf{E}_0 e^{-i\omega t}$, giving

$$\mathbf{r}(\omega) = -\frac{e/m}{\omega_0^2 - \omega^2 - i\omega/\tau} \mathbf{E}(\omega). \tag{1.7}$$

The polarization has the following relationship with the electric susceptibility (which we will simply denote by χ, since magnetic susceptibility is not of our concern here):

$$\mathbf{P} = Ne\mathbf{r} = \epsilon_0 \chi \mathbf{E}, \tag{1.8}$$

where N is the number density of oscillators. Then the susceptibility is found to be

$$\begin{aligned} \chi &= \frac{Ne^2}{\epsilon_0 m} 1/(\omega_0^2 - \omega^2 - i\omega/\tau) \\ &\equiv \chi_1 + i\chi_2. \end{aligned} \tag{1.9}$$

The real and imaginary (electric) susceptibilities are

$$\begin{aligned} \chi_1 &= \frac{Ne^2}{\epsilon_0 m} \frac{\omega_0^2 - \omega^2}{(\omega_0^2 - \omega^2)^2 + (\omega/\tau)^2}, \\ \chi_2 &= \frac{Ne^2}{\epsilon_0 m} \frac{\omega/\tau}{(\omega_0^2 - \omega^2)^2 + (\omega/\tau)^2}. \end{aligned} \tag{1.10}$$

Example (Brendel-Bormann oscillator model). There is another more sophisticated model for modelling the electric susceptibility inside matter called the **Brendel-Bormann oscillator model**. This model takes into account the effects of the local field around the oscillators and provides a more accurate description of the nonlinear optical response of materials.

This model does not give rise to any nonlinear effects or deviations. In the first days of the advent of laser, researchers observed unexpected phenomena that could not be explained by the Lorentz model, namely that unknown frequencies were shooting out of crystal samples.

However, when the electric field becomes strong enough, the assumption that fields obey harmonic relations is no longer valid. The nonlinear effects can be accounted by introducing higher order terms in the potential, which we will demonstrate with a x^2 term in the potential of a 1D system. Then

$$\frac{\mathrm{d}^2 x}{\mathrm{d}t^2} + \frac{1}{\tau}\frac{\mathrm{d}x}{\mathrm{d}t} + \omega_0^2 x + \alpha x^2 = -\frac{1}{m} F(t). \tag{1.11}$$

We shall assume for now that the electric field is strong enough for nonlinear effects to emerge, but not too strong such that it still lies in the **perturbative regime**.

Note. When are nonlinear (anharmonic) effects important? This question can be answered with a simple estimation. We will assume $\omega_0 \gg \omega_1, \omega_2$, so that

$$x \approx \frac{\omega_{0^2}}{\alpha} \tag{1.12}$$

and the atomic binding electric field is

$$E_{\text{atom}} = \frac{m\omega_0^4}{\alpha}. \tag{1.13}$$

1.2 Second-Order Nonlinear Effects

When the intensity of electromagnetic waves, or light beams, exceed a certain threshold, effects not describable by the linear Maxwell equations come into play.

We introduced the nonlinear correction term P_{NL} previously, now we will express the nonlinear contribution to polarization as a series of contracted tensors.

$$\begin{aligned} \mathbf{P}(t) &= \epsilon_0 \chi^{(1)} \mathbf{E}(t) + \mathbf{P}_{\text{NL}}(t) \\ &\equiv \epsilon_0 \chi^{(1)} \mathbf{E}(t) + \mathbf{P}^{(1)} + \mathbf{P}^{(2)} + \cdots \end{aligned} \tag{1.14}$$

Each polarization can be expressed in terms of the electric field using the appropriate susceptibility tensor:

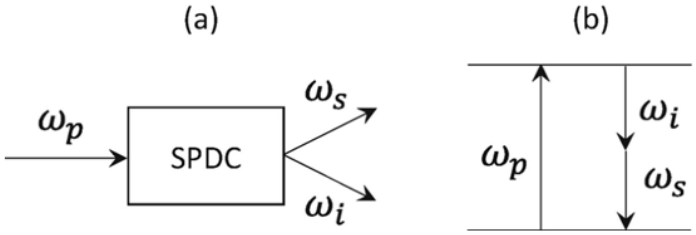

Figure 1.2: Illustration of the SPDC process.

$$\begin{aligned}\mathbf{P}^{(1)} &= \epsilon_0 \chi^{(1)} \mathbf{E}(t), \\ \mathbf{P}^{(2)} &= \epsilon_0 \chi^{(2)} \mathbf{E}(t)\mathbf{E}(t), \\ \mathbf{P}^{(3)} &= \epsilon_0 \chi^{(3)} \mathbf{E}(t)\mathbf{E}(t)\mathbf{E}(t), \\ &\vdots\end{aligned} \tag{1.15}$$

1.2.1 Sum- and Difference-Frequency Generation

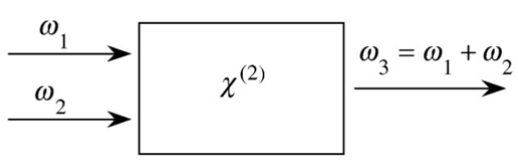

(a) Schematic diagram of sum-frequency generation (SFG).

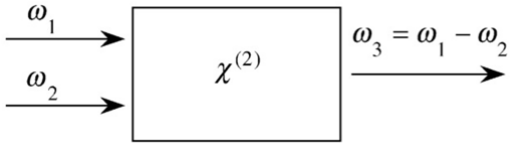

(b) Schematic diagram of difference-frequency generation (DFG).

Figure 1.1

1.2.2 Rectification

Note (Creation of Tera-Hertz EM Waves). As an example of application, rectification can be used to generate Tera-Hertz electromagnetic waves.

1.2.3 Second Harmonic Generation

1.2.4 Spontaneous Parametric Down-Conversion

Spontaneous parametric downconversion (SPDC) is a second-order optical process in which a single high energy photon (a pump photon) splits into two daughter photons of lower energies (conventionally known as the signal and idler photons) [Boy20]. It is a purely quantum process, so a complete treatment would require a full quantum description of the electromagnetic field.

1.3 Third-Order Nonlinear Effects

For noncentro-symmetric media, potential walls have both even and odd powers of position x. Therefore, third-order effects are ubiquitous in materials, while second-order effects are only present in special materials where the symmetry of the potential allows for an even-powered correction. Here we shall list a few important examples of third-order effects.

1.3.1 DC Kerr Effect

$$\chi^{(3)} = \chi^{(3)}(\omega_1 : \omega_1, 0, 0). \tag{1.16}$$

1.3.2 Self-Phase Modulation

This effect describes the interaction of a light wave with its own electric field, leading to a change in the wave's phase and frequency. It is a key mechanism in the generation of supercontinuum light, which we will mention later.

1.4 Symmetry and the Epsilon Tensor

Date: 20250911 The epsilon tensor of lossless media is **hermitian** .

1.5 Supercontinuum Generation

Spectral broadening and the generation of new frequency components are inherent features of nonlinear optics, and have been studied intensively since the early 1960s. One particular case is supercontinuum generation (SC), which occurs when narrow-band incident pulses undergo extreme nonlinear spectral broadening to yield a broadband, often a spectrally continuous white light.

1.5.1 Nonlinear Schrödinger Equation

The nonlinear Schrödinger equation (NLSE) is a fundamental equation in nonlinear optics that describes the evolution of slowly varying envelopes of optical pulses in a nonlinear medium. It takes the form:

$$i\frac{\partial A}{\partial z} + \frac{1}{2k_0}\nabla^2 A + \frac{n_2}{c}|A|^2 A = 0 \tag{1.17}$$

where A is the envelope of the optical field, k_0 is the linear wavevector, n_2 is the nonlinear refractive index, and c is the speed of light.

For light propagating in an optical fiber, we can include significant dispersion effects in the generalized nonlinear Schrödinger equation (GNLSE):

$$\frac{\partial A}{\partial z} + \frac{\alpha}{2}A + \sum_{m\geq 2}\frac{i^{\,m+1}\beta_m}{m!}\frac{\partial^{\,m} A}{\partial T^{\,m}} = i\gamma\left(1 + \frac{i}{\omega_0}\frac{\partial}{\partial T}\right)\left[A(T)\int_{-\infty}^{\infty} R(T')\,|A(T-T')|^2\,dT'\right]. \tag{1.18}$$

This equation takes into accounts the main effects taking place in a fiber during supercontinuum generation: Raman scattering, self-phase modulation, cross-phase modulation, four wave mixing, self-steepening, and dispersion. Raman scattering is considered a **delayed effect** , while the rest are **instantaneous** $\chi^(3)$**-effects** .

1.5.2 Self-Phase Modulation

1.5.3 Cross-Phase Modulation

1.5.4 Four-Wave Mixing

Four-wave mixing between continuous waves (CW) waves is one of the most fundamental processes in nonlinear optics. In the absence of any initial seeding (what does this mean?), four-wave mixing corresponds to an instability of the propagating CW pump, and growth from noise of sidebands symmetric in frequency about the pump can be observed.

Four-wave mixing and modulation instability are fequency- and time-domain description of identical physics.

1.5.5 Self-Steepening

1.5.6 Raman Scattering

Soliton fission

1.5.7 Dispersion

1.5.8 Simulation

When making simulations on the SCG effect, just as in the case of any quantitative simulations, the correct colormap should be chosen. In particular, the `jet` colormap is not perceptually uniform, i.e. the color transitions are not evenly spaced from a human perception perspective, and may lead to false features in the plot.

The code is based on code given in [DGC06]. First a separate function is defined to propagate the light through the fiber with the GNLSE, given by equation (1.18).

```
function [Z, AT, AW, W] = gnlse(T, A, w0, gamma, betas, ...
                                loss, fr, RT, flength, nsaves)

n = length(T); dT = T(2)-T(1); % grid parameters
V = 2*pi*(-n/2:n/2-1)'/(n*dT); % frequency grid
alpha = log(10.^(loss/10));    % attenuation coefficient

B = 0;
for i = 1:length(betas)        % Taylor expansion of betas
  B = B + betas(i)/factorial(i+1).*V.^(i+1);
end
L = 1i*B - alpha/2;            % linear operator

if abs(w0) > eps               % if w0>0 then include shock
    gamma = gamma/w0;
    W = V + w0;                % for shock W is true freq
else
    W = 1;                     % set W to 1 when no shock
end

RW = n*ifft(fftshift(RT.'));   % frequency domain Raman
L = fftshift(L); W = fftshift(W); % shift to fft space

% === define function to return the RHS of Eq. (3.13)
function R = rhs(z, AW)
  AT = fft(AW.*exp(L*z));          % time domain field
  IT = abs(AT).^2;                 % time domain intensity
  if (isscalar(RT)) || (abs(fr) < eps) % no Raman case
    M = ifft(AT.*IT);              % response function
  else
    RS = dT*fr*fft(ifft(IT).*RW); % Raman convolution
    M = ifft(AT.*((1-fr).*IT + RS));% response function
  end
  R = 1i*gamma*W.*M.*exp(-L*z);    % full RHS of Eq. (3.13)
end

% === define function to print ODE integrator status
function status = report(z, ~, flag) %
  status = 0;
  if isempty(flag)
    fprintf('%05.1f %% complete\n', z/flength*100);
  end
end

% === setup and run the ODE integrator
Z = linspace(0, flength, nsaves);  % select output z points
% === set error control options
options = odeset('RelTol', 1e-5, 'AbsTol', 1e-12, ...
                 'NormControl', 'on', ...
                 'OutputFcn', @report);
[Z, AW] = ode45(@rhs, Z, ifft(A), options); % run integrator

% === process output of integrator
AT = zeros(size(AW(1,:)));
for i = 1:length(AW(:,1))
  AW(i,:) = AW(i,:).*exp(L.'*Z(i)); % change variables
  AT(i,:) = fft(AW(i,:));           % time domain output
  AW(i,:) = fftshift(AW(i,:)).*dT*n;  % scale
end

W = V + w0; % the absolute frequency grid
```

```
end
```

Then the desired plots are generated with the appropriate parameters. Dispersion coefficients up to 9th order are included in the simulation, with the 9th-order term taking on a value as small as $-1.7140e-144$.

```
% === numerical grid ===
n = 2^13;                       % number of grid points
twidth = 12.5e-12;              % width of time window [s]
c = 299792458;                  % speed of light [m/s]
wavelength = 835e-9;            % reference wavelength [m]
w0 = (2*pi*c)/wavelength;       % reference frequency [Hz]
dt = twidth/n;
T = (-n/2:n/2 - 1).*dt; % time grid

% === input pulse ===
power = 10000;                  % peak power of input [W]
t0 = 28.4e-15;                  % duration of input [s]
A = sqrt(power)*sech(T/t0); % input field [W^(1/2)]

% === fibre parameters ===
flength = 0.15;                 % fibre length [m]
% betas = [beta2, beta3, ...] in units [s^2/m, s^3/m ...]
betas = [-1.1830e-026, 8.1038e-041, -9.5205e-056,  2.0737e-070, ...
         -5.3943e-085,  1.3486e-099, -2.5495e-114,  3.0524e-129, ...
         -1.7140e-144];
gamma = 0.11;                   % nonlinear coefficient [1/W/m]
loss = 0;                       % loss [dB/m]

% === Raman response ===
fr = 0.18;                      % fractional Raman contribution
tau1 = 0.0122e-12; tau2 = 0.032e-12;
RT = (tau1^2+tau2^2)/tau1/tau2^2*exp(-T/tau2).*sin(T/tau1);
RT(T<0) = 0;                    % heaviside step function

% === simulation parameters ===
nsaves = 200;     % number of length steps to save field at

% propagate field
[Z, AT, AW, W] = gnlse(T, A, w0, gamma, betas, loss, ...
                       fr, RT, flength, nsaves);

% === plot output ===
figure();
WL = 2*pi*c./W; iis = (WL>450e-9 & WL<1350e-9); % wavelength grid
lIW = 10*log10(abs(AW).^2 .* 2*pi*c./WL'.^2); % log scale spectral intensity
mlIW = max(max(lIW));           % max value, for scaling plot

ax1 = subplot(1,2,1);
C = lIW(:,iis);
C = C - max(C, [], 'all');                  % now max(C) = 0 dB
pcolor(ax1, WL(iis).*1e9, Z, C);
shading(ax1,'interp');
clim(ax1, [-40, 0]); xlim([450,1350]);
xlabel(ax1, 'Wavelength / nm'); ylabel(ax1, 'Distance / m');
colormap(ax1, turbo);
cb = colorbar(ax1,'eastoutside');
cb.Label.String = 'Spectral intensity (dB rel. max)';
set(gca,'YDir','normal','TickDir','out'); axis tight
cb.Ticks = -40:10:0;

lIT = 10*log10(abs(AT).^2); % log scale temporal intensity
mlIT = max(max(lIT));
ax2 = subplot(1,2,2);
pcolor(ax2, T.*1e12, Z, lIT);    % plot as pseudocolor map
clim(ax2, [mlIT-40.0, mlIT]);
xlim(ax2, [-0.5,5]);
shading interp;
xlabel('Delay / ps'); ylabel('Distance / m');
colormap(ax2, turbo);
cb = colorbar(ax2,'eastoutside');
cb.Label.String = 'Spectral intensity (dB rel. max)';
cb.Ticks = -40:10:0;
```

1.6 Nonlinear Interaction Reduce Noise

Example (Three modes with filter).

$$\begin{aligned}\text{Noise} &= \begin{pmatrix}\alpha_1^* & \alpha_2^* & \alpha_3^* & \alpha_1 & \alpha_2 & \alpha_3\end{pmatrix}\begin{pmatrix}0 & 0 & 0 & c_1+1 & c_2 & c_3\\ 0 & 0 & 0 & c_4 & c_5+1 & c_6\\ 0 & 0 & 0 & c_7 & c_8 & c_9+1\\ c_1 & c_2 & c_3 & 0 & 0 & 0\\ c_4 & c_5 & c_6 & 0 & 0 & 0\\ c_7 & c_8 & c_9 & 0 & 0 & 0\end{pmatrix}\begin{pmatrix}\alpha_1^*\\ \alpha_2^*\\ \alpha_3^*\\ \alpha_1\\ \alpha_2\\ \alpha_3\end{pmatrix} \\ &= (2c_1+1)|\alpha_1|^2 + (2c_5+1)|\alpha_2|^2 + (2c_9+1)|\alpha_3|^2 \\ &\quad + 2\text{Re}\left[c_2\alpha_1^*\alpha_2 + c_3\alpha_1^*\alpha_3 + c_4\alpha_2^*\alpha_1 + c_6\alpha_3^*\alpha_2 + c_7\alpha_3^*\alpha_1 + c_8\alpha_3^*\alpha_2\right].\end{aligned} \tag{1.19}$$

The terms with moduli squared are the vacuum fluctuations, and the cross terms are the correlations between different modes. If we apply a filter that blocks out mode α_3, then the noise becomes

$$\text{Noise}' = (2c_1+1)|\alpha_1|^2 + (2c_5+1)|\alpha_2|^2 + 2\text{Re}\left[c_2\alpha_1^*\alpha_2 + c_4\alpha_2^*\alpha_1\right]. \tag{1.20}$$

Chapter 2

Ultrafast Optics

2.1 Ultra-Short Pulses

Table 2.1: The colors of the visible light spectrum

Color	Wavelength interval	Cycle time interval
Red	∼700–635 nm	∼2.3–2.1 fs
Orange	∼635–590 nm	∼2.1–2.0 fs
Yellow	∼590–560 nm	∼2.0–1.9 fs
Green	∼560–520 nm	∼1.9–1.7 fs
Cyan	∼520–490 nm	∼1.7–1.6 fs
Blue	∼490–450 nm	∼1.6–1.5 fs
Violet	∼450–400 nm	∼1.5–1.3 fs

The swiftest chemical reaction known (radiolysis of water) is about 46 fs, while the average chemical reaction is about 200 fs. A ray of light travels about 0.3 μm in one femtosecond, approzimately the diameter of a virus.

2.2 Laser

Laser is the acronym for **Light Amplification by Stimulated Emission of Radiation**.

2.2.1 Poisson Distribution

Photons from a stable laser source can be appropriately described by a Poisson distribution, since the number of photons arriving at an ideal detector in a given time interval is a random variable. The Poisson distribution is defined as:

$$\text{Pois}(n;\lambda) = \frac{\lambda^n e^{-\lambda}}{n!} \tag{2.1}$$

where n is the number of photons detected and λ is the average number of photons arriving in the time interval.

2.3 Noise in Optical Systems

Noise can be quantified using various metrics, including the signal-to-noise ratio (SNR), which compares the level of the desired signal to the level of background noise. In optical systems, noise can arise from various sources, including thermal fluctuations, shot noise, and electronic noise.

Main classes of noise in the literature include: shot noise, quantum noise, thermal noise, flicker noise, and phase-sensitive/insensitive noise.

2.4 Optical Parametric Amplifier

An OPA process is responsible for the amplification of ultrafast laser pulses.

2.5 Structure of NOPA

Chapter 3

Numerical Methods

3.1 Runge-Kutta Methods

3.1.1 Classical Runge-Kutta Method

The **Classical Runge-Kutta method** is a widely used technique for solving ordinary differential equations (ODEs). It is a single-step method, meaning that it uses information from the current time step to compute the solution at the next time step.

The method is based on the idea of approximating the solution by evaluating the derivative at several points within the interval and taking a weighted average of these slopes. The classical Runge-Kutta method is often referred to as the 4th-order method, as it achieves a local truncation error of $O(h^5)$ and a global error of $O(h^4)$.

The method can be summarized in the following steps:

1. Given an initial value problem of the form

$$\frac{dy}{dt} = f(t, y), \quad y(t_0) = y_0,$$

   we want to compute $y(t_0 + h)$ for a small step size h.

2. Compute the following intermediate slopes:

$$\begin{aligned} k_1 &= hf(t_n, y_n), \\ k_2 &= hf\left(t_n + \frac{1}{2}h, y_n + \frac{1}{2}k_1\right), \\ k_3 &= hf\left(t_n + \frac{1}{2}h, y_n + \frac{1}{2}k_2\right), \\ k_4 &= hf\left(t_n + h, y_n + k_3\right). \end{aligned} \tag{3.1}$$

3. Update the solution using a weighted average of the slopes:

$$y_{n+1} = y_n + \frac{1}{6}(k_1 + 2k_2 + 2k_3 + k_4). \tag{3.2}$$

3.1.2 Runge-Kutta-Fehlberg Method

The **Runge-Kutta-Fehlberg (RKF) method** , also known as simply the Fehlberg method, is a popular adaptive step size method. It estimates the local truncation error and adjusts the step size accordingly.

It can be formulated as either a fourth-order or fifth-order method, and is particularly useful for solving ordinary differential equations where the solution may change rapidly. The recursive solutions are

$$y_{n+1}^{(4)} = y_n + \frac{25}{216}k_1 + \frac{1408}{2565}k_3 + \frac{2197}{4104}k_4 - \frac{1}{5}k_5 \tag{3.3}$$

and

$$y_{n+1}^{(5)} = y_n + \frac{16}{135}k_1 + \frac{6656}{12825}k_3 + \frac{28561}{56430}k_4 - \frac{9}{50}k_5 + \frac{2}{55}k_6, \tag{3.4}$$

where the k_i values are defined as follows:

$$
\begin{aligned}
k_1 &= h\, f(t_n, y_n), \\
k_2 &= h\, f\left(t_n + \frac{1}{4}hy_n + \frac{1}{4}k_1\right), \\
k_3 &= h\, f\left(t_n + \frac{3}{8}hy_n + \frac{3}{32}k_1 + \frac{9}{32}k_2\right), \\
k_4 &= h\, f\left(t_n + \frac{12}{13}hy_n + \frac{1932}{2197}k_1 - \frac{7200}{2197}k_2 + \frac{7296}{2197}k_3\right), \\
k_5 &= h\, f\left(t_n + hy_n + \frac{439}{216}k_1 - 8k_2 + \frac{3680}{513}k_3 - \frac{845}{4104}k_4\right), \\
k_6 &= h\, f\left(t_n + \frac{1}{2}hy_n - \frac{8}{27}k_1 + 2k_2 - \frac{3544}{2565}k_3 + \frac{1859}{4104}k_4 - \frac{11}{40}k_5\right).
\end{aligned}
\tag{3.5}
$$

The Butcher tableau for the Fehlberg 4(5) method (RKF45) is shown in table 3.1.

c_i	a_{i1}	a_{i2}	a_{i3}	a_{i4}	a_{i5}	a_{i6}
0						
$\frac{1}{4}$	$\frac{1}{4}$					
$\frac{3}{8}$	$\frac{3}{32}$	$\frac{9}{32}$				
$\frac{12}{13}$	$\frac{1932}{2197}$	$-\frac{7200}{2197}$	$\frac{7296}{2197}$			
1	$\frac{439}{216}$	-8	$\frac{3680}{513}$	$-\frac{845}{4104}$		
$\frac{1}{2}$	$-\frac{8}{27}$	2	$-\frac{3544}{2565}$	$\frac{1859}{4104}$	$-\frac{11}{40}$	
	$\frac{25}{216}$	0	$\frac{1408}{2565}$	$\frac{2197}{4104}$	$-\frac{1}{5}$	0
	$\frac{16}{135}$	0	$\frac{6656}{12825}$	$\frac{28561}{56430}$	$-\frac{9}{50}$	$\frac{2}{55}$

Table 3.1: Butcher tableau for the Runge–Kutta–Fehlberg 4(5) method.

3.2 Automatic Differentiation

Three main methods of calculating derivatives are: numeric differentiation, symbolic differentiation, and **automatic differentiation (AD)**. Automatic differetiation is a powerful technique that allows for the efficient and accurate computation of derivatives of functions, particularly in the context of machine learning and optimization.

Numeric differentiation approximates derivatives using finite differences, which can introduce numerical errors. Symbolic differentiation manipulates mathematical expressions to derive exact formulas, this solves the issue of numerical inaccuracies and instabilities but can be computationally expensive for complex functions. The leading issue for symbolic differentiation is *expression swell*, where the size of the expression grows exponentially with the number of operations, making it impractical for large functions.

Example (Expression in Composite Functions)**.** The function

$$f(x) = \frac{e^{wx+b} + e^{-(wx+b)}}{e^{wx+b} - e^{-(wx+b)}} \tag{3.6}$$

has a symbolic derivative of

$$\frac{\partial f}{\partial w} = \frac{(-xe^{-b-wx} - xe^{b+wx})(e^{-b-wx} + e^{b+wx})}{(-e^{-b-wx} + e^{b+wx})^2} + \frac{-xe^{-b-wx} + xe^{b+wx}}{-e^{-b-wx} + e^{b+wx}}. \tag{3.7}$$

Automatic differentiation, on the other hand, computes derivatives by applying the chain rule to the operations in a function, allowing for efficient and accurate derivative calculations.

3.3 Adjoint Method in Optics Design

The nonlinear adjoint method can be applied to general (nonlinear) objective functions and sources of nonlinearity, allowing for the design of novel nonlinear optical devices.

The goal of inverse design is to find a set of real-valued design variables that maximize a real-valued objective function $\mathcal{L} = \mathcal{L}(\mathbf{E}, \mathbf{E}^\star, \phi)$. In linear systems, $\mathbf{E}$ is a complex-valued vector corresponding to the electric field solution of the (linear) Maxwell equations. In the nonlinear case, $\mathbf{E}$ may be interpreted more generally as the solution to a nonlinear equation

$$F(\mathbf{E}, \mathbf{E}^\star, \phi) = 0. \tag{3.8}$$

The solution to equation (3.8) can be found with the Newton-Raphson method, which has a complexity of $\mathcal{O}(N^2)$, where N is the number of design variables $\dim(\phi)$.

3.4 Stochastic Differential Equations

The state of the art method for solving quantum noise problems is through solving **stochastic differential equations (SDEs)** . The SDEs are often used to model systems influenced by random noise, such as quantum systems subject to thermal fluctuations or other forms of stochastic perturbations.

Chapter 4

Ultrashort Pulse Characterization

4.1 Frequency-Resolved Optical Grating

Frequency-resolved optical gating (FROG) is a technique for the complete characterization of ultrashort pulses. It measures not only pulse parameters such as the pulse energy or pulse duration, but also the full time-dependent electric field, including the optical spectrum[Pas]. This method allows us to measure an ultrashort laser pulse without a shorter reference pulse [<**empty citation**>].

A sophisticated iterative phase retrieval algorithm, implemented with a computer program, can then be used for reconstructing the pulse shape from the FROG trace.

4.2 Cross-Correlation Frequency Optical Grating

really. It uses the spectrally resolved cross-correlation signal of the weak pulse with a fully characterized reference pulse to generate a spectrogram, which is analyzed by an iterative algorithm. No spectral overlap between unknown and reference pulse is needed, which makes this method very flexible.

Chapter 5

Applications

5.1 Ultrafast Optics in Biophysics

5.2 Ultrafast Optics in Condensed Matter Physics

Appendix

Appendix A

To Be Added

Bibliography

[Boy20] Robert W. Boyd. *Nonlinear Optics*. 4th ed. Academic Press (Elsevier), 2020, p. 608. ISBN: 978-0-12-811003-4. DOI: 10.1016/C2018-0-02977-9.

[DGC06] John M. Dudley, Goëry Genty, and Stéphane Coen. "Supercontinuum generation in photonic crystal fiber". In: *Rev. Mod. Phys.* 78 (4 Oct. 2006), pp. 1135–1184. DOI: 10.1103/RevModPhys.78.1135. URL: https://link.aps.org/doi/10.1103/RevModPhys.78.1135.

[Pas] Rüdiger Paschotta. *xfrog*. https://www.rp-photonics.com/frequency_resolved_optical_gating.html. Accessed: 2025-07-27.